The NLO corrections to W^+W^-Z production at the LHC

Dao Thi Nhung, Le Duc Ninh, Marcus Weber (arXiv:1307.7403) | 14 August 2013

Institut für Theoretische Physik

Outline

Karlsruher Institut für Technologie

1. Motivation
2. Calculation Framework
   - NLO QCD
   - NLO EW
3. Results
4. Conclusions

Motivations

Karlsruher Institut für Technologie

Why W^+W^-Z production at the LHC?

- It is posible to access this mechanism at the upgraded LHC
- It is a signal process for the study $W^+W^-Z\gamma$, W^+W^-ZZ couplings
- It is a backgound process for new physics studies

Motivations

Why W^+W^-Z production at the LHC?

- It is posible to access this mechanism at the upgraded LHC
- It is a signal process for the study $W^+W^-Z\gamma$, W^+W^-ZZ couplings
- It is a backgound process for new physics studies

Why NLO accuracy is important?

- LO results suffer from large theoretical uncertainty
- QCD correction is of $\mathcal{O}(100\%)$ Hankele et. at. (2007), T, Binoth et. al.(2008)
- EW correction is also significant, especially in high transverse momentum regime due to the Sudakov effects.
- Studying QCD and EW corrections help us understanding about quantum effects

Motivations

Why W^+W^-Z production at the LHC?

- It is posible to access this mechanism at the upgraded LHC
- It is a signal process for the study $W^+W^-Z\gamma$, W^+W^-ZZ couplings
- It is a backgound process for new physics studies

Why NLO accuracy is important?

- LO results suffer from large theoretical uncertainty
- QCD correction is of $\mathcal{O}(100\%)$ Hankele et. at. (2007), T, Binoth et. al.(2008)
- EW correction is also significant, especially in high transverse momentum regime due to the Sudakov effects.
- Studying QCD and EW corrections help us understanding about quantum effects

This talk gives the full picture of NLO prediction to this process

Tree level estimation

Partonic cross section is of $\mathcal{O}(\alpha^3_{G_\mu})$ order. We include:

- $q\bar{q} \to W^+W^-Z$, $q = u, d, c, s$: $>90\%$

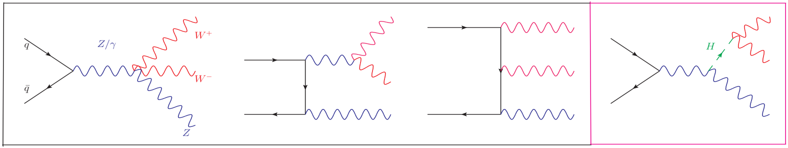

- $b\bar{b} \to W^+W^-Z$: about 2.5 %
- $\gamma\gamma \to W^+W^-Z$: about 5 %

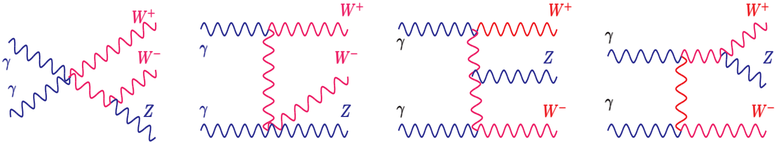

NLO QCD corrections to $q\bar{q} \to W^+W^-Z$

- Virtual: only light quarks and gluon in loops (five-point tensor integral rank 4)

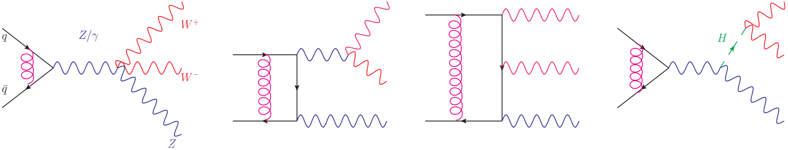

- Real gluon: g attached to the quark line
  - gluon radiation: gluon in the final state
  - gluon induced: gluon in the initial state

NLO QCD corrections to $q\bar{q} \to W^+W^-Z$

- Virtual: only light quarks and gluon in loops (five-point tensor integral rank 4)

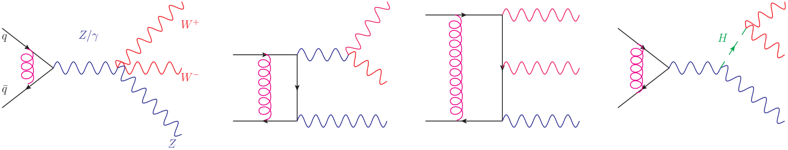

- Real gluon: g attached to the quark line
  - gluon radiation: gluon in the final state
  - gluon induced: gluon in the initial state
- Regulating UV divergences by dimensional regularization, quark masses and quark fields are renormalized on-shell ($\delta m_q = 0$)
- Soft and collinear singularities arising from the splitting $q \to q^* g$ and $g \to q^* \bar{q}$ regulated by two methods:
  - Dimensional regularization: using Catani-Seymour algorithm, $4 \to D = 4 - 2\epsilon$, (singularities $1/\epsilon, 1/\epsilon^2$)
  - Mass regularization: using Dittmaier's subtraction formula, *i.e.* introduce mass regulator for quark and gluon, (singularities $\log(m^2), log^2(m^2)$)

translation between two methods: $\log(m^2) \to \frac{1}{\epsilon} - \gamma_E + \log(4\pi\mu^2)$. Numerical agreement within statistic error.

NLO EW corrections to $q\bar{q} \to W^+W^-Z$

- Virtual contribution: $\gamma, W^{\pm}, Z, H$ in loops and a fermion loop ($q = u, d, c, s, b, t$), many structures $\to$ more complicated
- Real photon contributions: γ attached to quark line, W line or WWZ/γ vertices
  - photon radiation: photon in the final state
  - photon induced: photon in the initial state
- e, M_W, M_Z, M_H and external wave functions are renormalized in on-shell scheme. Using Fermi constant G_μ as input parameter,

$$\delta Z_e = -\frac{1}{2}\delta Z_{AA} - \frac{s_W}{2c_W}\delta Z_{ZA} - \frac{1}{2}\Delta r,$$

- Mass regularization is used to isolate IR singularities. Phase-space slicing method has been checked again dipole subtraction method: good agreement

Checks of the calculation

- Check UV, IR finiteness
- Two independent calculations are in good agreement
- Two independent loop integral libraries.
- One calculation uses: FeynArt, FormCalc, In-house LoopInts, Bases
- numerical instabilities occur in the numerical integration of the virtual corrections. Gram determinant checked at every phase-space point for N-point tensor coefficients (N=3,4)

$$\frac{\det(2p_i p_j)}{(2p_{\max}^2)^{N-1}} < 10^{-3}$$

  tensor coefficients are calculated with quadruple precision.
- Five-point tensor integrals: using Denner-Dittmaier method to avoid the small determinant problem.

Scale dependence

- Only QCD correction is studied
- Fix scale: $\mu = \mu_R = \mu_F, \mu_0 = (2M_W + M_Z)$
- Dynamic scale: $\mu = \mu_R = \mu_F, \mu_0 = M_{WWZ}$

$$\delta = \frac{|\sigma(2\mu_0) - \sigma(\mu_0/2)|}{\sigma(\mu_0)}$$

LO: 2.5% (Fix), 2.7% (Dyn)

NLO:12.2% (Fix), 10% (Dyn)

No better choice for the scale

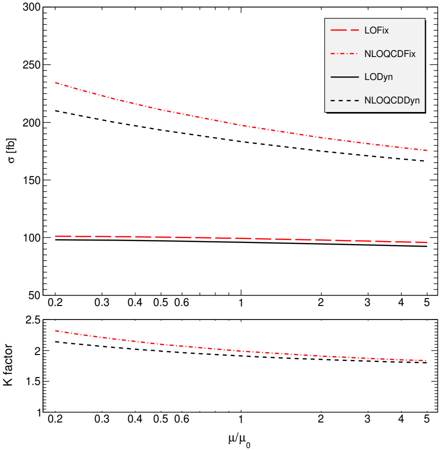

Total cross section

- LHC 14 TeV
- quark PDFs: MSTW2008
- photon PDFs: MRST2004qed

		Fixed scale		Dynamic scale	
		$\sigma[fb]$	$\delta[\%]$	$\sigma[fb]$	$\delta[\%]$
LO		99.29(2)	...	95.91(2)	...
$\bar{b}b$		2.4173	2.4	2.6915	2.8
$\gamma\gamma$		4.852	4.9	5.559	5.8
Δ_{QCD}	$q\bar{q}$	48.83(3)	49.2	53.33(3)	55.6
	$qg, \bar{q}g$	49.29(1)	49.6	34.07(1)	35.5
Δ_{EW}	$q\bar{q}$	-8.74(1)	-8.8	-8.05(1)	-8.4
	$q\gamma, \bar{q}\gamma$	6.81(1)	6.8	5.854(9)	6.1
Δ_{NLO}		103.46(4)	104.2	93.46(4)	97.4

P_T distributions

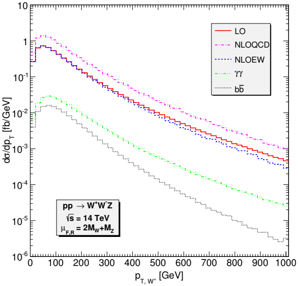

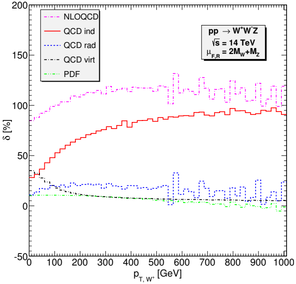

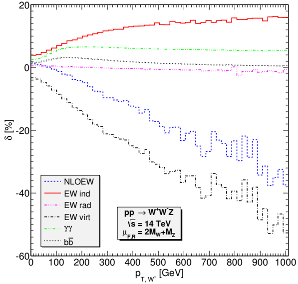

P_T distributions with jet-veto

- Fix jet veto: veto all events with $p_{T,j} > 25$ GeV and $\eta_j < 4.5$
- Dynamic jet veto: veto all events with $p_{T,j} > \max(M_{T,W^+}, M_{T,W^-}, M_{T,Z})/2$

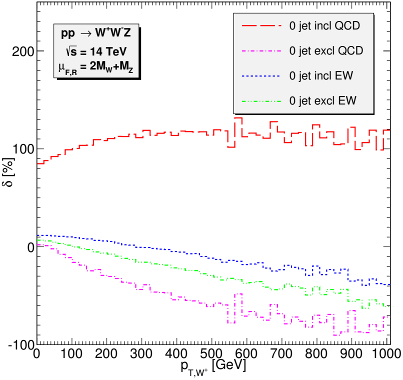

Fix jet veto

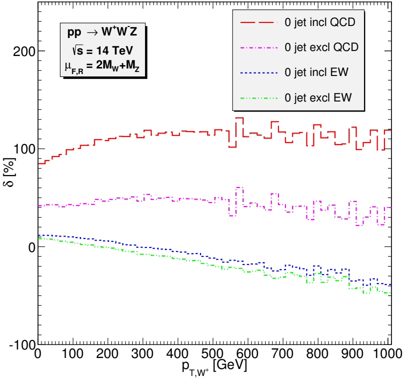

Dynamic jet veto

jet-veto with uncertainty

- Dynamic jet veto: veto all events with $p_{T,j} > \max(M_{T,W^+}, M_{T,W^-}, M_{T,Z})/2$
- Varying scale: $\frac{2M_W+M_Z}{2} < \mu < 2(2M_W + M_Z)$

- $\sigma_{0j,excl} = \sigma_{0j,incl} - \sigma_{1j,incl}$
- Black band: 0jet and 1jet inclusives are fully correlated

$$\Delta_{0j,excl} = \Delta_{0j,incl} - \Delta_{1j,incl}$$

- Purple band: two observables are uncorrelated
  Stewart and Tackmann, 2011

$$\Delta^2_{0j,excl} = \Delta^2_{0j,incl} + \Delta^2_{1j,incl}$$

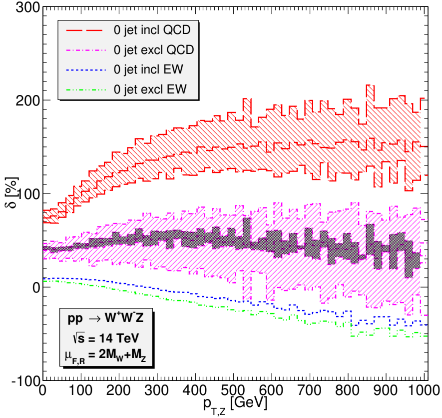

Conclusions

Karlsruher Institut für Technologie

- Full NLO EW correction has been calculated for the first time
- EW correction is of 2% at cross section level
- EW correction has large impact on the p_T distribution of gauge boson. Mount to -30% at large p_T
- NLO QCD correction has been calculated. k-factor is large and not a constant. NLO QCD correction increases scale dependence
- Using dynamic jet veto renders the QCD correction to moderate but almost unchanges the EW correction

Conclusions

Karlsruher Institut für Technologie

- Full NLO EW correction has been calculated for the first time
- EW correction is of 2% at cross section level
- EW correction has large impact on the p_T distribution of gauge boson. Mount to -30% at large p_T
- NLO QCD correction has been calculated. k-factor is large and not a constant. NLO QCD correction increases scale dependence
- Using dynamic jet veto renders the QCD correction to moderate but almost unchanges the EW correction

THANK YOU FOR YOUR ATTENTION